# Characterization of 3D Printed Highly Filled Composite: Structure, Thermal Diffusivity and Dynamic-Mechanical Analysis

Antonella Patti[a,*], Gianluca Cicala[a], Claudio Tosto[a], Lorena Saitta[a], Domenico Acierno[b]

[a] Department of Civil Engineering and Architecture (DICAr), University of Catania, Viale Andrea Doria 6,95125 Catania, Italy
[b] CRdC Nuove Tecnologie per le Attività Produttive Scarl,Via Nuova Agnano 11, 80125, Naples, Italy
antonella.patti@unict.it

This study focuses on the characterization of 3D printed parts by fused deposition modelling (FDM) technique made from a composite filament, highly loaded of stainless-steel microparticles, prepared at different infill density (0, 50, 100%). Thermo-mechanical properties, morphological aspects and heat transport behaviour of the developed specimens have been investigated by dynamic-mechanical analysis (DMA), thermal diffusivity measurements and scanning electron microscopy (SEM). Experimental results allowed to attest a drastic reduction of storage modulus in the range of testing temperatures by reducing the infill density. In the meantime, an increment of dissipation factor was shown in lesser stiff samples at temperatures near to the ambient. The same increasing trend did not appear in the case of thermal diffusion that showed closer values for samples at 0 and 50% of infill, and an augment in the case of infilling level of 100%. This outcome, explained through SEM pictures, was attributed to the difficulty in realization of perfect empty internal structures within 3D parts. A supporting analysis by IR spectroscopy was conducted on the composite surface to gain qualitative information about constituting polymer filament. Further considerations on the porosity of systems have been obtained elaborating SEM micrographs with ImageJ software.

## 1. Introduction

Nowadays, a versatile and promising technology has gained the interest of academic and industrial communities given the easy fabrication of complex three-dimensional objects by following the layer-by-layer deposition: the so-called Additive Manufacturing (AM) process. Several materials as metals, ceramics, plastics or composites can be processed by adopting different AM methods, even if the most common among them is the AM extrusion (i.e. Fused Filament Fabrication (FFF), Fused Deposition Modeling (FDM), Robocasting). Recently, also highly filled (HF) polymer formulations, incorporating metal or ceramic particles, have been experimented (Tosto et al., 2021). For example, two different types of iron-based powders (stainless steel 316L and pure iron) have been added (mass fraction of 41.4%) to polylactic acid (PLA) for promising biodegradable implants in bone tissue engineering (Jiang et al., 2021). The mechanical properties of 3D printed products resulted to be strongly affected by infill design such as layer thickness, infill pattern, infill density, infill width, and infill deposition speed. Generally, the higher the infill density, the greater the tensile and compressive strength (Suteja and Soesanti, 2020). Yet, the main reason to reduce the infill density in 3D parts (less than 100% infill) was the consequential reduction in printing time, energy and material cost (Ćwikła et al., 2017). Furthermore, a critical aspect of this technology that limited the performance of 3D printed parts compared to that achieved by other manufacturing methods, was the development of inherent defects during the production process as void formation, surface roughness and poor bonding between fibre and matrix (Wickramasinghe et al., 2020). In regard, in the work of Liao et al. (2019), the effect of porosity and crystallinity on the final properties of PLA-based 3D printed specimens has been reported. Morphological observations highlighted the creation of numerous pores in the specimens' cross-sections.

Experimental results showed anisotropic features in tested products, attributed to the occurrence of orientation during the layer deposition and the creation of order and disorder structures. The authors proposed a thermal treatment to optimize the crystallinity and avoid anisotropy. Stepashkin et al. (2018) prepared composite systems, made from carbon fiber (CF) and polyether ether ketone (PEEK), by novel FDM methodology, and studied the corresponding features in terms of thermal conductivity and microscopic images. Testing demonstrated the fiber orientation along polymer flow inducing the anisotropy of thermal properties, and the presence of crack and defects attributed to thermal and mechanical stress during the filament deposition.

In this work, a commercial metal/polymer composite, in form of filament, was processed by fused deposition modelling and characterized in terms of thermal diffusivity and dynamic mechanical properties. The effect of different infill density (0, 50, 100% of infill) on the tested parameters has been investigated. Final considerations on morphological aspects and IR spectroscopy have been also reported.

## 2. Materials and Methods

A commercial filament of stainless-steel-composite material (Ultrafuse 316L), supplied by BASF (Ludwigshafen, Germany), has been introduced in a 3D printing machine (mod. M200) produced by Zortrax (Olsztyn, Poland), and processed in the following conditions: i) temperature of 240°C and 90°C for the nozzle and bed, respectively; ii) nozzle diameter of 0.4 mm, ii) retraction distance of 2 mm and retraction speed of 40 mm/sec; iii) layer height of 0.09 mm. The samples have been realized by setting 0, 50, and 100% of infill degree.

Attenuated total reflection (ATR) analyses performed on the filament material by using a Fourier transform infrared (FTIR) spectrophotometer (mod. Spectrum 100) produced by PerkinElmer (Massachusetts, United States), endowed with an optical crystal, made from diamond. The measurements were performed within a wavenumber range of 600–4000 $cm^{-1}$, with a resolution of 4 $cm^{-1}$ and 16 scans for each sample. The collected data have been reworked by performing baseline correction and advanced ATR correction, related to the adopted crystal, by OMNIC software.

Thermal diffusivity of developed specimens, square in size (side of 12.7 mm and thickness of 2 mm), was measured by adopting LFA 467 HT HyperFlash machine (Netzsch, Germany). The operation mode of the device was the so-called non-steady-state conditions, consisting of a flashlight source crossing the sample through-thickness in a bottom-up direction. In the upper part, a liquid nitrogen-cooled IR detector was placed. The area of the analyzed sample was equal to 70%, the measurement was repeated 3 times, and the Cowen model was used for fitting the signal. The thermal diffusivity was evaluated by adopting the following formula (1):

$$Thermal\ diffusivity = \frac{1.38\ d^2}{t_{1/2}} \tag{1}$$

where d is the sample's thickness and $t_{1/2}$ is the time required for the signal to reach 50% of its maximum value.(Gaal et al., 2004)

The dynamic-mechanical analyses (DMA) of 3D printed parts have been performed on an instrument (mod. Tritec 2000), realized by Triton Technology Ltd. (Leicestershire, UK). Rectangular specimens ($15\times3.5\times3.2$ $mm^3$) have been tested in tension mode at frequencies of 1 Hz at a heating rate of 2 °C/min, starting from room temperature to 160 °C.

An emission scanning electron microscope (SEM EVO by Zeiss, Oberkochen, Germany), operating in high vacuum conditions has been used for analyzing the sample cross-section after the gold metallization.

## 3. Experimental Results

### 3.1 IR spectroscopy

Infrared spectroscopy (IR) is an extremely useful technique that allows the identification of possible polymer based-species present in tested materials. Results of IR analysis, performed on the virgin filament (Ultrafuse 316L), have been reported in terms of absorbance vs wavenumbers ($cm^{-1}$) in the range from 4000 to 600 $cm^{-1}$. In the following Figure 1, characteristic well visible peaks were highlighted: 1) at 2981 and 2922 $cm^{-1}$ corresponded to the symmetric stretching of $CH_2$ groups; 2) at 1236 $cm^{-1}$ correlated to the twisting of methylene group; 3) at 1092 $cm^{-1}$ related to the C-O-C asymmetric stretching, and finally 4) at 903 $cm^{-1}$ to the C-O-C symmetric stretching. All these vibration modes were intended as an indication of specific molecular bonding typical of polyoxymethylene (POM) monomer. (Król-Morkisz et al., 2019)
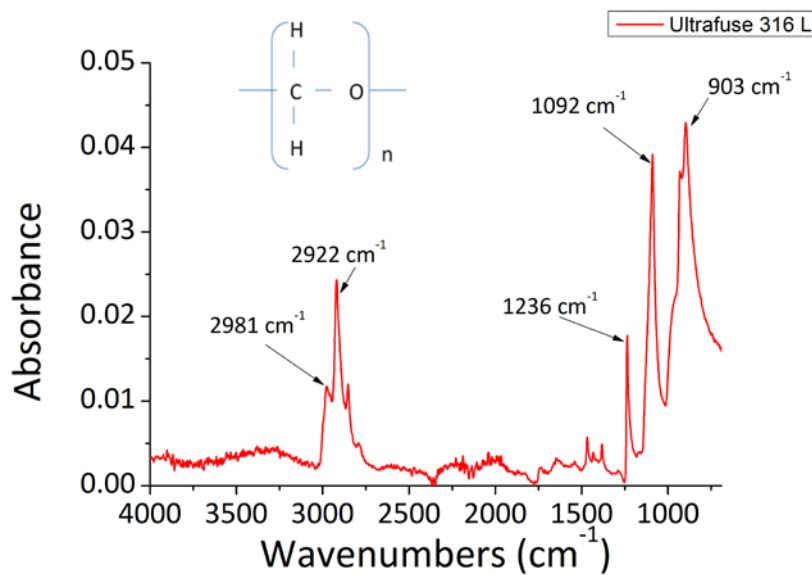
*Figure 1 ATR spectrum for Ultrafuse 316 L*

### 3.2 Thermal diffusivity

In Table 1, the thermal diffusivity of 3D printed samples by Ultrafuse 316 L filament has been reported in function of sample characteristics, *i.e.* the different percentage of infill equal to 0, 50, 100%, respectively. In the case of the lowest infill value (0%), the heat diffusion was measured equal to 0.217 mm$^2$/sec. A small negligible increment (+7%) was verified in correspondence of samples at 50% of infill. By growing the level of filling up to 100% in printed specimens, the thermal diffusivity achieved a value equal to 0.384 mm$^2$/sec, corresponding to an increment of about 77% compared to the tested parameter in the absence of filling (0%). Depending on the technical datasheet, the filament composition is represented by 80 wt.% (~42 vol.%) of steel and 20 wt.% (58 vol%) of polymer ("BASF Ultrafuse 316L | 3Kg," n.d.). Taking into account the literature data (Osswald and Hernández-Ortiz, 2006), the first constituent possesses a thermal diffusivity of 1.41 mm$^2$/sec, while that of the second (being potentially POM) is 0.07 mm$^2$/sec. So, given these considerations, and according to the rule of mixtures theory, the thermal diffusion in filled samples realized with the chosen filament material (80% steel, 20% POM) should correspond to 0.632 mm$^2$/sec. On the contrary, in this case, a drastic reduction (~39%) seemed to be evident by considering the measured value at 100% of infill. This result led to attest that the heat conduction in 3D prepared samples, even if at the maximum allowable filling conditions, was much lower than potential achievable values, given the intrinsic thermal ability of constituents and their compositions in the filament. In the work of Zhao et al. (2004), the authors studied the thermal transport in highly porous cellular metal foam using a combined experimental and analytical approach, by highlighting the effect of pore size and porosity on the ability of heat conduction inside developed metal foams. According to this consideration, besides all the other aspects affecting the thermal conduction in a traditional composite (i.e. interfacial resistance (Russo et al., 2018) and dispersion (Patti et al., 2016)), it could be supposed that the presence of defect and porosity inside the samples promoted a strong deterioration of heat transport inside the material.

*Table 1:Thermal diffusivity of developed samples at different infill percentage.*

| Sample Infill | Thermal diffusivity (mm$^2$/sec) |
| --- | --- |
| 0% | 0.217 |
| 50% | 0.233 |
| 100% | 0.384 |

### 3.3 Dynamic Mechanical Analysis (DMA)

Experimental results of thermo-mechanical properties were shown in Figure 2, in terms of Storage Modulus (Pa) and dissipation factor (tan delta) curves as a function of temperature.
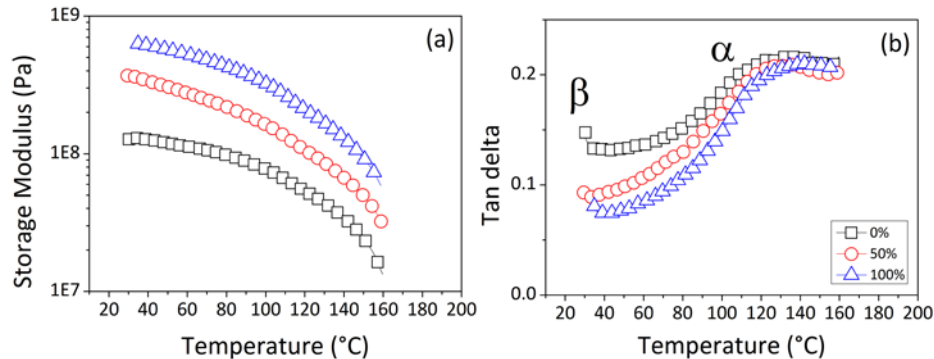


*Figure 2 Storage modulus (a) and damping factor (b) as a function of temperature at 1 Hz for 3D printed parts. Legend in Figure 2b as in 2a.*

From data of storage modulus, a decreasing trend was evident by increasing the temperature for all investigated specimens. For the system at 0% of infill, the storage modulus started at room temperature from a value around $10^8$ Pa, an order of magnitude lower value compared to composites at 100% of infill (~$10^9$ Pa), and collapsed to approximately $10^7$ Pa at 160°C. The storage modulus curve of systems at 50% infill remained exactly located in all the tested range of temperatures between two others.

As concerning the dissipation factor, all samples showed the same trend: they started from higher values at room temperature, then during the heating, decreased and afterwards rose again by achieving a peak around 0.2 in correspondence of 130°C. This tendency was associated with the typical relaxation zones ($\gamma, \beta, \alpha$) of the POM polymer. In details, the $\gamma$ zone takes place from -70 and -50°C and is related to the glass transition. In the temperature range between -50 and 50°C, the $\beta$ zone arises from a cooperative glass-transition motion, due to the movement of non-crystalline segments inhibited by crystallite surface. Finally, the $\alpha$ zone, starting close to 60°C, is considered due to the crystalline phase mobility and relaxation of intensity is ascribed to early melting of defective crystals or "premelting" of POM (Keating et al., 1997). Yet, in the range of temperatures between 20 and 80°C, it could be highlighted that the tan delta of samples at lower infill was superior to systems at 100% of infill. This aspect was attributed to the greater ability in energy dissipation developed in lesser stiff materials.(Aw et al., 2018)

### 3.4 Morphological Aspects

In the following Figure 3, the SEM imagines of samples at 0% of infill and two different magnifications (a) 50X and (b) 300X, and at 100% of infill (c) 50X and (d) 300X, have been reported. As easily predictable, the first specimens appeared with a superior degree of internal porosity, associated both to the established process parameters and to the possible defects derived from the 3D printing technologies. While the first type could be intended as macro-porosity, being in the order of magnitude of millimetre scale, the second one could be considered micro-porosity, falling in the range of magnitude of micrometre scale. By the imagines, it could be also detected that the value of infilling equal to zero was quite impossible to be obtained because the Zortrax machine fixed by default a minimum value of top and bottom layers that cannot be fixed down to one layer only. Then, during the melted material deposition, once the inferior base was realized, the filaments, involved in the upper surface, were collapsed under the effect of the weight, making it impossible to build a totally hollow structure in the central part.By elaborating SEM micrographs through ImageJ software, a characterization of micro-porosity was evaluated through the distribution of defects or void in function of the corresponding area and the so-called parameter, pseudo-sphericity (how the shape was closer to a perfect sphere), for each tested specimen. From data, shown in Figure 4, it could be observed that for materials at 0% of an infilling level, the most voids possessed an area inferior to 30 µm$^2$ and shape close to circular objects (pseudo-sphericity ~0.9), whereas for materials at 100% of an infilling level, a greater surface seemed to be involved in the space in the range between 1-50 µm2 with also a more irregular shape (pseudo-sphericity~0.2).
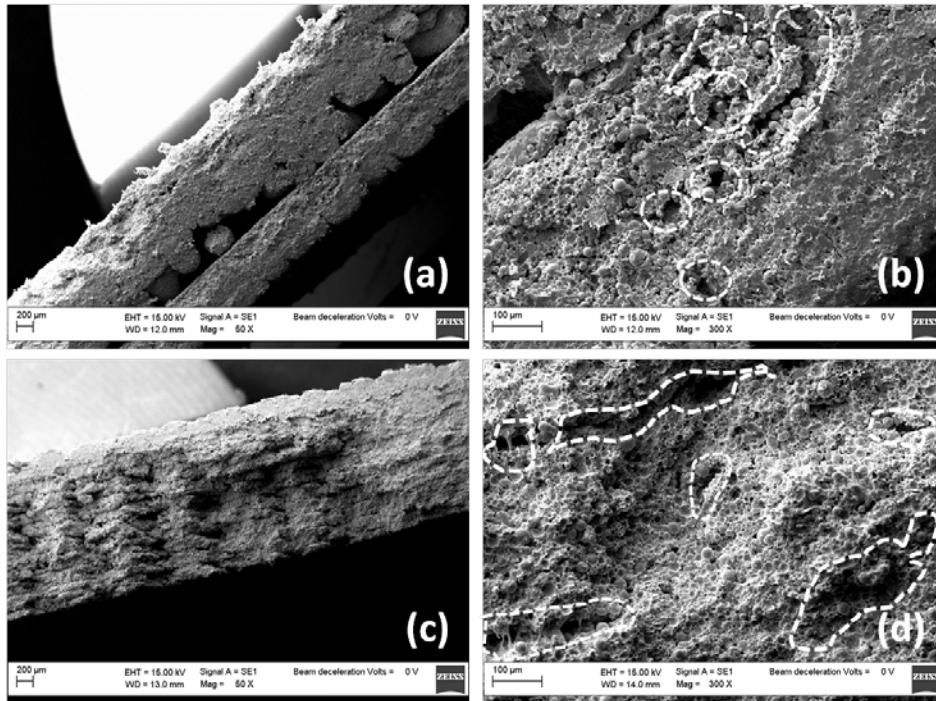
*Figure 3 SEM micrographs of samples cross-section at infill of 0% (magnification of 50X (a) and 300X (b)) and infill of 100% (magnification of 50X (c) and 300X (d)).*
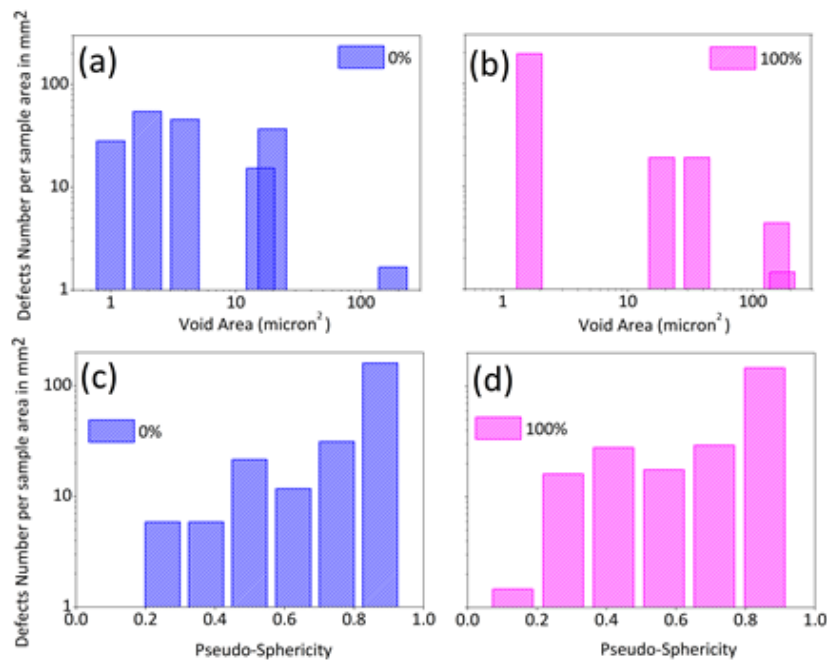


*Figure 4 Number of void/defects per unit of sample area in mm$^2$ vs Void area (a) at 0% and (b) 100% of infilling level, or vs the pseudo-spherical shape (c) at 0% and (d) 100% of infilling level.*

## 4. Conclusions

In this work, a characterization of 3D printed samples, at different infill (0, 50, 100%), made from a commercial filament processed through FDM technology, was presented mainly in terms of thermal diffusivity and DMA

analysis. From the experimental data, by increasing the infill level the storage modulus of developed specimens was increased, whereas the ability in energy dissipation was lowered, especially at temperatures near the ambient. On the contrary, the thermal diffusivities of samples at 0% and 50% of infilling level were very close to each other. Then, an increase of 77% in thermal diffusivity was verified in correspondence of infill level of 100% compared to 0 %. Finally, SEM pictures highlighted sample microstructure characterized by different types of porosity: the first induced by infilling level (macro-porosity) and the second derived from the manufacturing process (micro-porosity).

## Acknowledgments

## References

Aw, Y.Y., Yeoh, C.K., Idris, M.A., Teh, P.L., Hamzah, K.A., Sazali, S.A., 2018, Effect of Printing Parameters on Tensile, Dynamic Mechanical, and Thermoelectric Properties of FDM 3D Printed CABS/ZnO Composites, Materials, 11, 466–480.

BASF Ultrafuse 316L | 3Kg [WWW Document], n.d. URL https://www.crea3d.com/it/basf/643-736-basf-ultrafuse-316l-3kg.html (accessed 3.3.21).

Ćwikła, G., Grabowik, C., Kalinowski, K., Paprocka, I., Ociepka, P., 2017, The influence of printing parameters on selected mechanical properties of FDM/FFF 3D-printed parts. In: IOP Conference Series: Materials Science and Engineering. Institute of Physics Publishing, pp. 12033–12043.

Gaal, P.S., Thermitus, M.A., Stroe, D.E., 2004, Thermal conductivity measurements using the flash method, Journal of Thermal Analysis and Calorimetry, 78, 185–189.

Jiang, D., Ning, F., Wang, Y., 2021, Additive manufacturing of biodegradable iron-based particle reinforced polylactic acid composite scaffolds for tissue engineering, Journal of Materials Processing Technology 289, 116952–116964.

Keating, M.Y., Sauer, B.B., Flexman, A.E., 1997, Dynamic mechanical characterization of relaxations in poly(oxymethylene), miscible blends, and oriented filaments, Journal of Macromolecular Science, Part B: Physics, 36, 717–732.

Król-Morkisz, K., Karaś, E., Majka, T.M., Pielichowski, K., Pielichowska, K., 2019, Thermal stabilization of polyoxymethylene by PEG-functionalized hydroxyapatite: Examining the effects of reduced formaldehyde release and enhanced bioactivity, Advances in Polymer Technology, 2019, 1–17.

Liao, Y., Liu, C., Coppola, B., Barra, G., Di Maio, L., Incarnato, L., Lafdi, K., 2019, Effect of Porosity and Crystallinity on 3D Printed PLA Properties, Polymers, 11, 1487–1501.

Osswald, T., Hernández-Ortiz, J.P., 2006, Polymer Processing Modeling and Simulation, Hanser Publishers, Munich, Germany.

Patti, A., Russo, P., Acierno, D., Acierno, S., 2016, The effect of filler functionalization on dispersion and thermal conductivity of polypropylene/multi wall carbon nanotubes composites, Composites Part B, Engineering, 94, 350–359.

Russo, P., Patti, A., Petrarca, C., Acierno, S., 2018, Thermal conductivity and dielectric properties of polypropylene-based hybrid compounds containing multiwalled carbon nanotubes, Journal of Applied Polymer Science, 135, 46470–46479.

Stepashkin, Chukov, D.I., Senatov, F.S., Salimon, A.I., Korsunsky, A.M., Kaloshkin, S.D., 2018, 3D-printed PEEK-carbon fiber (CF) composites: Structure and thermal properties, Composites Science and Technology, 164, 319–326.

Suteja, T.J., Soesanti, A., 2020, Mechanical Properties of 3D Printed Polylactic Acid Product for Various Infill Design Parameters: A Review. In: Journal of Physics: Conference Series. Institute of Physics Publishing, pp. 42010–42016.

Tosto, C., Tirillò, J., Sarasini, F., Cicala, G., 2021, Hybrid metal/polymer filaments for fused filament fabrication (FFF) to print metal parts. Applied Sciences, 11, 1444–1458.

Wickramasinghe, S., Do, T., Tran, P., 2020, FDM-Based 3D Printing of Polymer and Associated Composite: A Review on Mechanical Properties, Defects and Treatments, Polymers, 12, 1529–1571.

Zhao, C.Y., Kim, T., Lu, T.J., Hodson, H.P., 2004, Thermal transport in high porosity cellular metal foams. Journal of Thermophysics and Heat Transfer, 18, 309–317.